International Journal of Mineral Processing 130 (2014) 74–81

Contents lists available at ScienceDirect

International Journal of Mineral Processing

journal homepage: www.elsevier.com/locate/ijminpro

# Thermal stress FEM analysis of rock with microwave energy

Yicai Wang, Nenad Djordjevic

*Julius Kruttschnitt Mineral Research Centre, The University of Queensland, Australia*

ARTICLE INFO

*Article history:*
Received 26 September 2013
Received in revised form 2 April 2014
Accepted 29 May 2014
Available online 6 June 2014

*Keywords:*
Thermal stress
Microwave energy
Numerical modelling
FEM
Cracks

ABSTRACT

This paper presents a study of a thermal breakage process used to analyse the thermal stress and crack development that occur when rock is exposed to short-pulse microwave energy. A two-dimensional circular plate, containing two-phase minerals, was used in finite element simulation to calculate thermal stress for the purpose of better understanding thermal fracture behaviour in comminution. It is found that the thermal mismatch between a microwave-absorbing inclusion and a low-absorbing matrix mineral can generate large localized thermal stresses around the inclusion. Fracture initially occurs, not around the grain boundaries between the two minerals, but some distance away, as a result of thermal expansion stress on the matrix mineral. The results also indicate that though grain size is one of the factors causing cracks during heating of granular materials, it is not the only reason. The size and the thermal properties of the matrix mineral can also affect the results of thermal stresses.



## 1. Introduction

Breakage is essential in most mineral processing operations to liberate valuable minerals. The comminution process in the mineral processing industry is extremely energy-intensive, accounting for the majority of energy consumption in the mineral recovery process (Schwechten and Milburn, 1990).

Heating to facilitate comminution has been applied in the mineral industry for nearly a century (Yates, 1918; Holman, 1926). In 1984 the microwave absorption properties of minerals were reported by Chen et al. (Chen, 1984). Their research indicated that certain groups of minerals, such as chalcopyrite, pyrite, galena and magnetite, are good heaters (microwave-absorbing); while others, such as silicate and carbonate gangue minerals, are poor heaters (microwave low-absorbing). Significantly, different thermal properties between different mineralogical species in the same rock result in the generation of thermal stresses and, consequently, cracks within the rock sample. Many studies on this subject have been published in the past two decades (Wills et al., 1987; Raddatz et al., 1989; Rowson and Rice, 1990; Uslu et al., 2003). Fitzgibbon and Veasey (1990) suggested that these thermal cracks may lead to a significant reduction in grinding resistance during the comminution process. Walkiewicz et al. (1991) postulated that rapid heating of microwave-absorbing minerals in low-absorbing material generated thermal stresses capable of causing micro-cracks along grain boundaries,

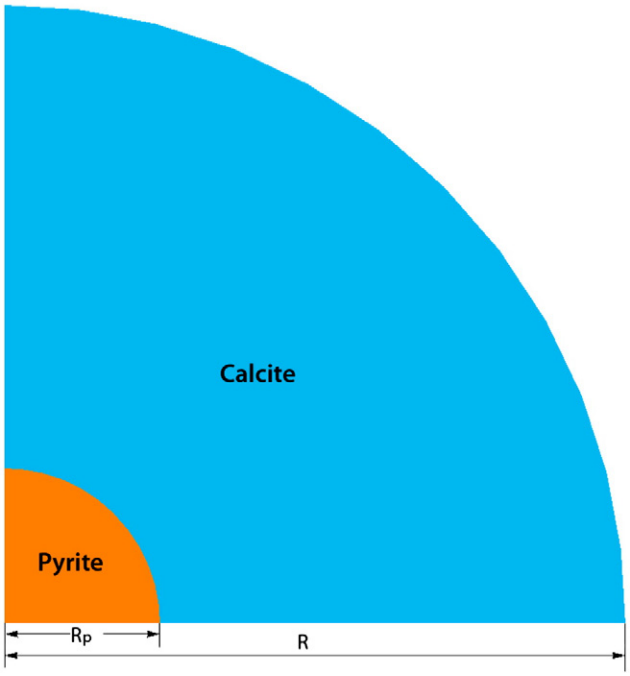


**Fig. 1.** A calcite matrix with one pyrite inclusion.

*E-mail address:* uqywang2@uq.edu.au (Y. Wang).

http://dx.doi.org/10.1016/j.minpro.2014.05.012
0301-7516/

**Table 1**
Mechanical properties.

| Mineral | Young's modulus (GPa) | Poisson ratio | Density (kg/m$^3$) |
|---|---|---|---|
| Calcite | 72.3 | 0.32 | 2680 |
| Pyrite | 292 | 0.16 | 5018 |

**Table 2**
Thermal properties in different temperatures.

| Thermal expansion coefficient ($\alpha \times 10^{-6}$) | | | |
|---|---|---|---|
| Mineral | 373 K | 473 K | 673 K |
| Calcite | 13.1 | 15.8 | 20.1 |
| Pyrite | 27.3 | 29.3 | 33.9 |
| *Thermal conductivity (W/m K)* | | | |
| Mineral | 273 K | 373 K | 500 K |
| Calcite | 4.02 | 3.01 | 2.55 |
| Pyrite | 37.9 | 20.5 | 17 |
| *Specific heat capacity (J/kg K)* | | | |
| Mineral | 298 K | 500 K | 1000 K |
| Calcite | 819 | 1051 | 1238 |
| Pyrite | 517 | 600 | 684 |

and that this type of micro-cracking might have the potential to improve both the grind ability of the ore and liberation of the individual mineral grains. They undertook a detailed quantitative study of the microwave heating characteristics of various minerals and compounds.

Salsman et al. (1996), Kingman and Rowson (1998), Jones et al. (2002, 2005), Haque (1999) and Amankwah et al. (2005) discussed the potential applications of microwave technology to comminution and mineral processing. Many authors, for example, Lindroth and Podnieks (1988) have suggested that rocks could be thermally weakened by the application of high power microwaves. Satish et al. (2006) investigated microwave-assisted breakage in a laboratory test.

Wang and Forssberg (2005) presented their experimental results to estimate the effect of microwave pre-heat. They demonstrated the effects of microwave energy intensity and exposure time on microwave heating behaviour and grind ability. Their results also indicated that particle size has a significant effect in microwave heating process.

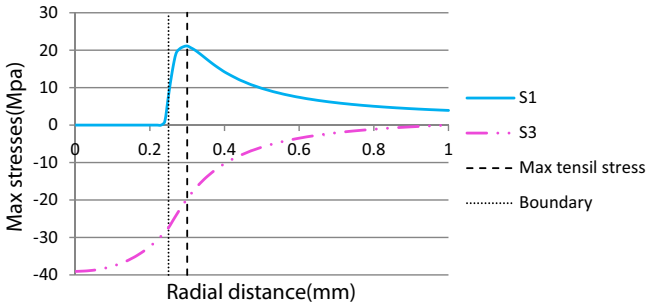


**Fig. 3.** Stresses as a function of radial distance for power density $P_d = 10^{11}$ W/m$^3$ with exposure time $t = 0.0007$ s.

The main advantage of using microwave technology is that only the high-absorbing minerals are affected by the applied energy with little energy wasted on the low-absorbing minerals.

Although thermal stress and thermal cracking have been studied for many years, numerical studies of the processes of crack initiation, propagation and linkage have not been undertaken to a great extent. Challenges need to be overcome through a fundamental understanding of how microwaves interact with minerals. The entire thermal cracking process is difficult to quantify by laboratory experiments alone.

The aim of this paper is to propose a thermal stress damage model that can numerically simulate the thermal cracking processes of initialization, propagation and coalescence. The results of the thermal mismatch between microwave-absorbing material and low-absorbing material on the stress distribution and crack development will be presented.

## 2. Basic concept

It is well known that dielectric materials can be heated by exposing them to high frequency electromagnetic fields and the amount of thermal energy deposited into an ore material due to microwave heating can be calculated as Eq. (1):

$$P_d = 2\pi f \varepsilon_0 \varepsilon_r'' E_0^2 \tag{1}$$

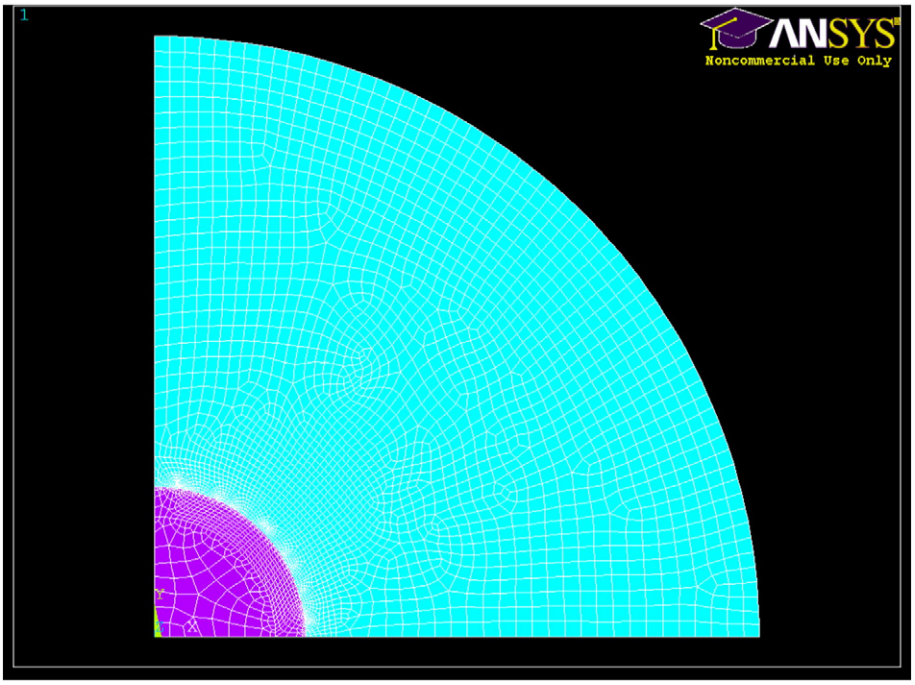


**Fig. 2.** Finite element mesh.

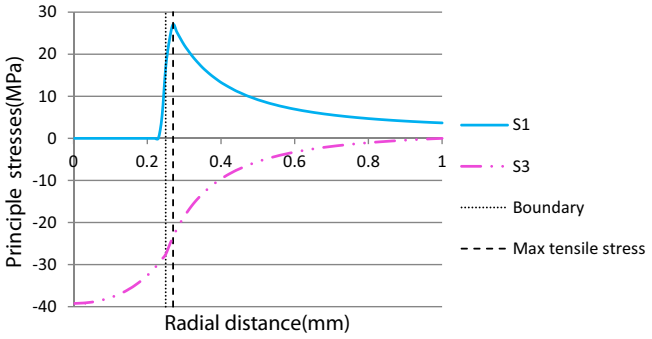


**Fig. 4.** Principle stresses without thermal expansion on calcite.

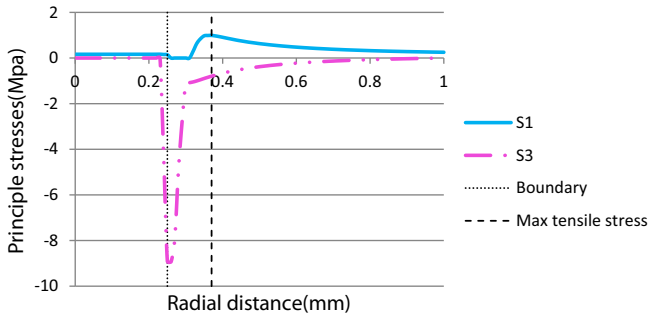


**Fig. 5.** Principle stresses without thermal expansion on pyrite.

where $P_d$ is the volumetric energy absorption density of the mineral ($W/m^3$), $f$ is the frequency of the microwave energy (2.45 GHz), $\varepsilon_0$ is the permittivity of free space ($8.854 \times 10^{-12}$ F/m), $\varepsilon_r$ is the dielectric loss factor of the mineral and $E_0$ is the magnitude of the electric field portion of the microwave energy (V/m).

The rise in temperature of the ore materials inside a microwave field can be calculated from the average power density described in Eq. (2):

$$C_p \rho_0 \frac{\partial T}{\partial t} = P_d + \nabla \cdot (k \nabla T) \tag{2}$$

where $\rho_0$ is the mineral density ($kg/m^3$), $C_p$ is the specific heat (J/kg·K) and $k$ is the thermal conductivity (W/(mK)) when a heat flow exists in the system.

In the microwave industry, it is easier to describe the energy using the term 'power density' ($W/m^3$), which is the amount of power (time rate of energy transfer) per unit volume. It can be converted to the traditional energy unit of (kWh/t) using Eq. (3) if the density of minerals is known (units are listed in brackets):

$$E = t \times P_d \times \frac{V}{m}\left(\frac{s \cdot W \cdot m^3}{m^3 \cdot kg}\right) = 2.78e^{-4} \times \frac{1}{\rho_0} \times P_d \left(\frac{kWh}{t}\right) \tag{3}$$

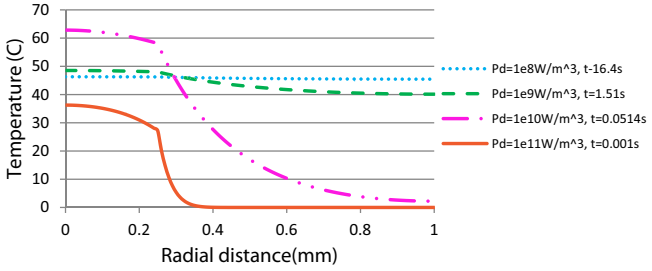


**Fig. 6.** Temperature for different power densities at the same level of principle stress.

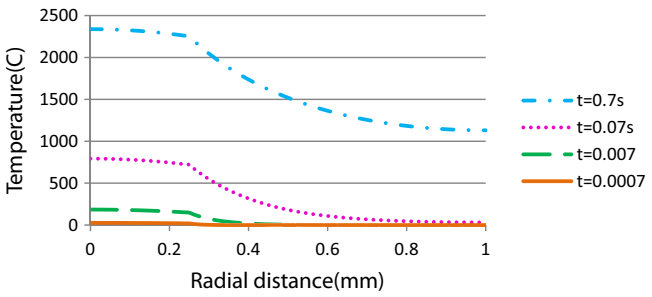


**Fig. 7.** Temperature for power density $P_d = 10^{11}$ W/m$^3$ with different exposure times.

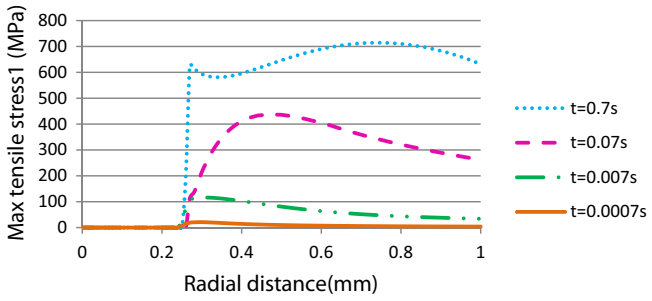


**Fig. 8.** Max tensile stress under a power density $P_d = 10^{11}$ W/m$^3$ with different exposure times.

where V ($m^3$) is the volume of mineral and m (kg) is the mass of the mineral.

In order to compare the results with those from other scholars, the term 'power density' will be used in this paper.

The total strain component in a whole sample is given by Eq. (4):

$$\varepsilon = \varepsilon^{\sigma} + \varepsilon^{T} \tag{4}$$

where $\varepsilon^{\sigma}$ is the strain caused by elastic stresses and $\varepsilon^{T}$ is the isotropic thermal strain induced by temperature change, in a two-dimensional case they can be expressed by Eqs. (5) and (6):

$$\varepsilon^{\sigma} = \begin{Bmatrix} \varepsilon_x \\ \varepsilon_y \\ \gamma_{xy} \end{Bmatrix} = \begin{bmatrix} \frac{\partial u}{\partial x} \\ \frac{\partial v}{\partial y} \\ \frac{\partial u}{\partial y} + \frac{\partial v}{\partial x} \end{bmatrix} = \begin{bmatrix} \frac{\partial}{\partial x} & 0 \\ 0 & \frac{\partial}{\partial y} \\ \frac{\partial}{\partial y} & \frac{\partial}{\partial x} \end{bmatrix} \begin{Bmatrix} u \\ v \end{Bmatrix}. \tag{5}$$

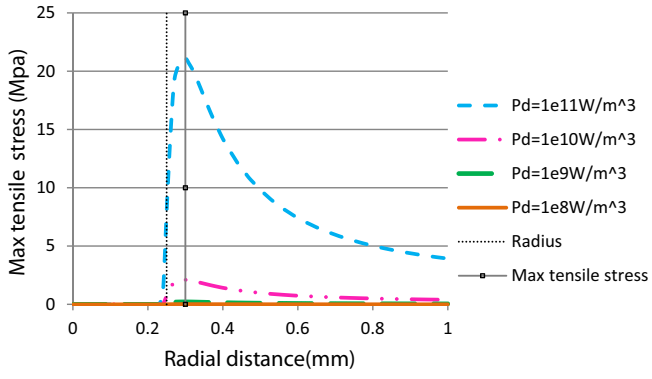


**Fig. 9.** Max tensile stress under different power densities with the same exposure time $t$ = 0.0006 s.

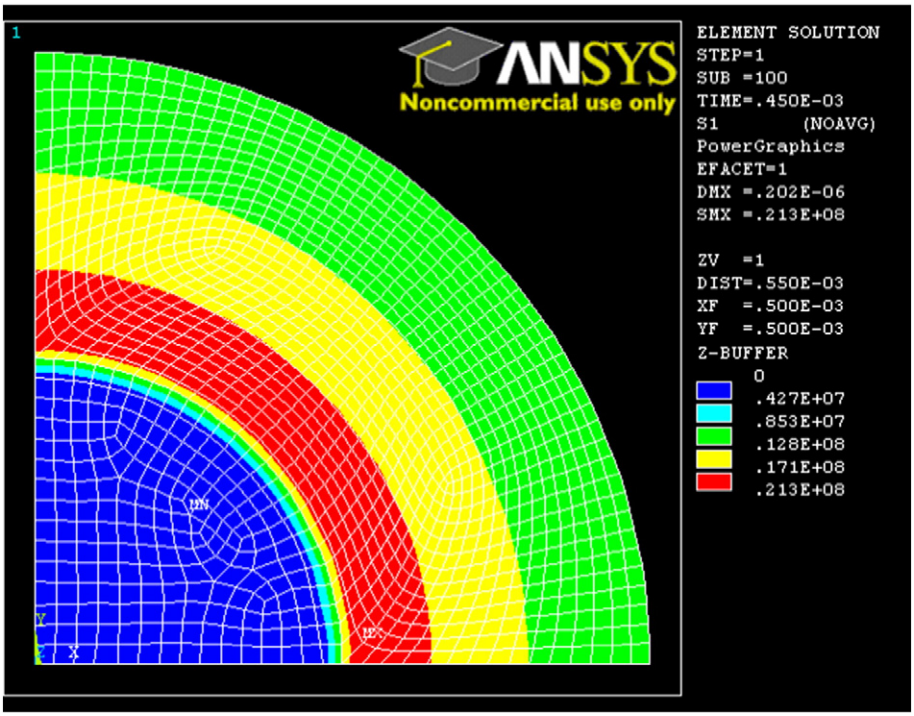


**Fig. 10.** Maximum tensile stress from ANSYS.

In which $u$ and $v$ are the displacements in the $x$ and $y$ directions respectively.

$$\varepsilon^T = \begin{Bmatrix} \varepsilon_x^T \\ \varepsilon_y^T \\ \gamma_{xy}^T \end{Bmatrix} \tag{6}$$

The stress can be derived from Eq. (7):

$$\{\sigma\} = [\mathrm{D}]\{\varepsilon\} \tag{7}$$

where [D] is the constitutive tensor. For plane stress, isotropic material, it is in the form of Eqs. (8) and (9):

$$[\mathrm{D}] = \frac{E}{1-\nu^2}\begin{bmatrix} 1 & \nu & 0 \\ \nu & 1 & 0 \\ 0 & 0 & \frac{1-\nu}{2} \end{bmatrix} \tag{8}$$

$$\varepsilon^T = \begin{Bmatrix} \alpha\Delta T \\ \alpha\Delta T \\ 0 \end{Bmatrix} \tag{9}$$

and for plane strain, isotropic material, it is in the form of Eqs. (10) and (11):

$$[\mathrm{D}] = \frac{E(1-\nu)}{(1+\nu)(1-2\nu)}\begin{bmatrix} 1 & \frac{\nu}{1-\nu} & 0 \\ \frac{\nu}{1-\nu} & 1 & 0 \\ 0 & 0 & \frac{1-2\nu}{2(1-\nu)} \end{bmatrix} \tag{10}$$

$$\varepsilon^T = (1+\nu)\begin{Bmatrix} \alpha\Delta T \\ \alpha\Delta T \\ 0 \end{Bmatrix} \tag{11}$$

where $\alpha$ is the thermal expansion coefficient and $\Delta T$ is the temperature increase.

## 3. Numerical model

A two-dimensional finite element model containing two minerals was constructed, in which a single disc-shaped grain of pyrite was surrounded by a larger disc of calcite. The geometry and materials are shown in Fig. 1. Pyrite and calcite were selected as typical minerals for the inclusion and host rock, respectively. The aims were to simulate the thermal stresses and the location of peak stress when the pyrite grain is exposed to high power microwave energy, and to test the effects of power density and grain size. The external boundary of the calcite matrix was assumed to be thermally insulated. Axial symmetry allows this geometry to be analysed in only one quadrant. The material properties of the minerals are listed in Tables 1 and 2.

The elastic properties of the minerals were measured by the micro-indentation method. From samples of AMARA GeM P843 project, the value of Young's Modulus for calcite is 72.3 GPa and the value from Mineral Database is 82 GPa, which is quite different to the values found in other papers 797 GPa (Salsman et al., 1996; Jones et al., 2005).

## 4. Results analysis and discussions

### 4.1. Stress distribution

The first numerical model, with $R_p = 0.25$ mm and $R = 1$ mm, was undertaken using the commercial software ANASYS. Fig. 2 shows the mesh on the model. Because the tensile strength of brittle material is much lower than compressive strength (generally one tenth), from the stress results in Fig. 3, it is obvious that at the initial cracking stage, maximum tensile stress (S1) is the major cause of damage. At radial distances $r < 0.25$ mm, i.e. within the pyrite particle, the thermal stresses are mainly compressive. The tensile stress occurs in the calcite matrix and the maximum value is at $r = 0.3$ mm, which is beyond the interface of the two minerals at $r = 0.25$ mm. This tensile stress can initiate cracks in the calcite matrix.

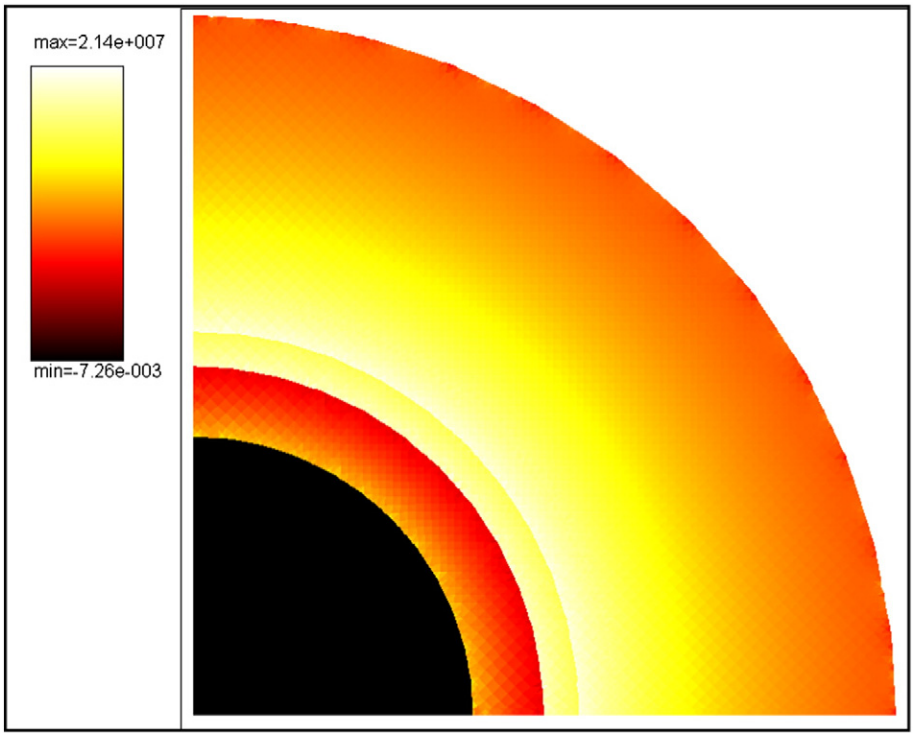


**Fig. 11.** Maximum tensile stress from the software of SimRock.

In order to investigate why the maximum stress location was away from the grain boundary, the thermal expansion coefficient of calcite was set to zero, which removed the effect of the thermal response of the calcite. The results in Fig. 4 show that the maximum tensile stress 1 (S1), in the absence of the thermal expansion of calcite, occurred very close to the grain boundary. It was also substantially higher than the maximum stress in Fig. 3 (27.1 MPa versus 21.0 MPa) because the temperature was kept in the mineral of pyrite. The thermal property of host rock (calcite) therefore significantly affects both the peak value of tensile stress and its location.

In another trial, the thermal expansion coefficient of pyrite was set to zero, in order to consider only the effect of the thermal expansion on calcite. Fig. 5 shows that both the thermal tensile and compressive stresses (S1 and S3) distributed over the whole sample were not large enough to change the breakage pattern. These results clearly indicate that the thermal expansion coefficient of the microwave-absorbing mineral (Pyrite) plays a critical role in producing thermal stresses and the location of initial cracking can be affected by the thermal property of the low-absorbing mineral (Calcite).

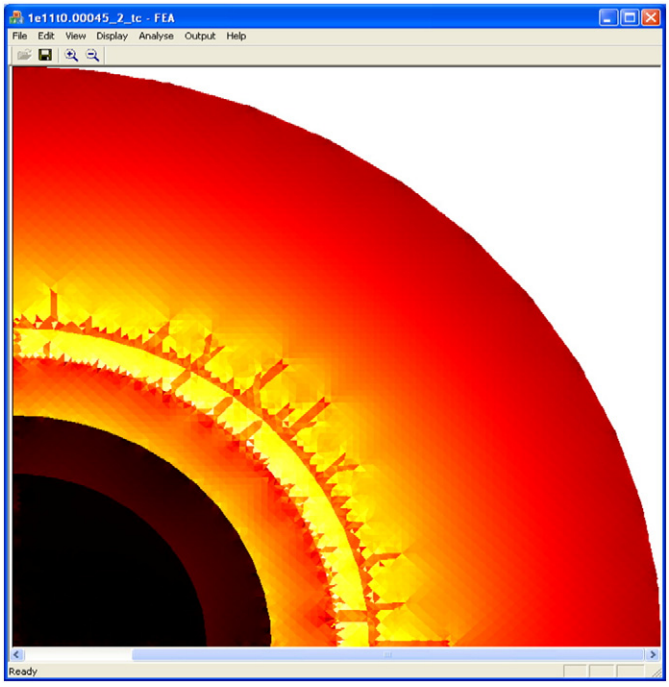


**Fig. 12.** Crack simulation from the SimRock software.

### 4.2. Effects of power density and pulse duration

Previously published work has revealed that short pulses of a very high power density can dramatically improve the economics of microwave assisted grinding (Wang, 2013).

Because the constituents of ore often have very different thermal and mechanical properties, such as large differences in thermal expansion coefficients, thermal stresses can far exceed the typical strengths of these materials during heating.

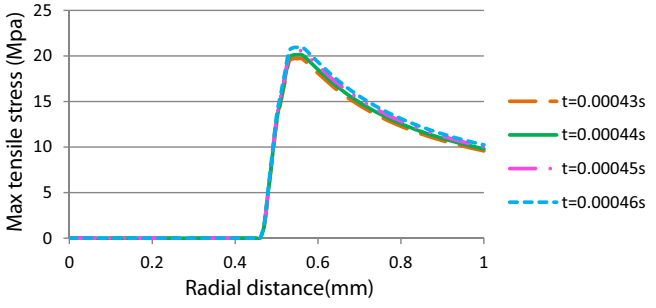


**Fig. 13.** Maximum tensile stress in different exposure times under power density $P_d = 10^{11}$ W/m$^3$.

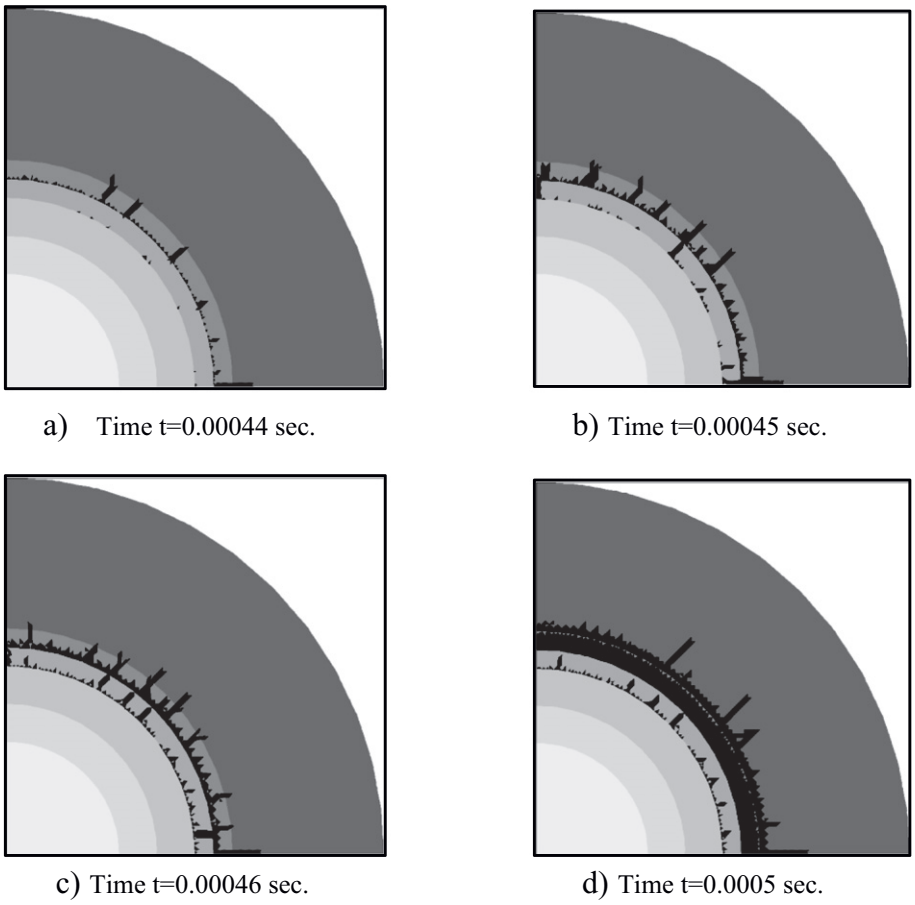


**Fig. 14.** Crack simulations at different exposure times.

Fig. 6 shows the thermal results for four different power densities, considered at different exposure times to produce the same maximum tensile stress level (approximately 28 MPa). For a lower power density level $P_d = 10^8$ W/m$^3$ or $P_d = 10^9$ W/m$^3$, a very flat temperature profile can be observed, which indicates that, for lower microwave energy even with a longer exposure of 16 s, the microwave-absorbing mineral is inappropriate.

Increasing the power densities to $P_d = 10^{10}$ W/m$^3$ or $P_d = 10^{11}$ W/m$^3$ greatly shortened the time required to obtain a similar stress level and provided a sharper temperature gradient. This means that for a high power density, especially $P_d = 10^{11}$ W/m$^3$, the time is too short to cause thermal diffusion in calcite, so most of the calcite remains very near its initial temperature, i.e. the energy is very efficiently used to produce the breakages. In these circumstances a high power density combined with a short heating interval would, therefore, maximize energy efficiency. Also the lower power density has a lower gradient of increase with temperature.

These conclusions can also be observed from Fig. 7, in which the same power density $P_d = 10^{11}$ W/m$^3$ is used over different time intervals. For the longest time $t = 0.7$ s, the thermal diffusion occurred in the calcite, and the lowest temperature in calcite reached 1130 °C.

The basic concept of microwave energy application in the mineral process is the thermal mismatch between minerals of microwave-absorbing inclusion and low-absorbing matrix, therefore, if the temperature in calcite is higher, much of the energy will be wasted.

The curves in Fig. 8 show that the maximum stress shifted well away from the pyrite over time. In mineral breakage, this location shift is undesirable because cracking in this location would not liberate the pyrite.

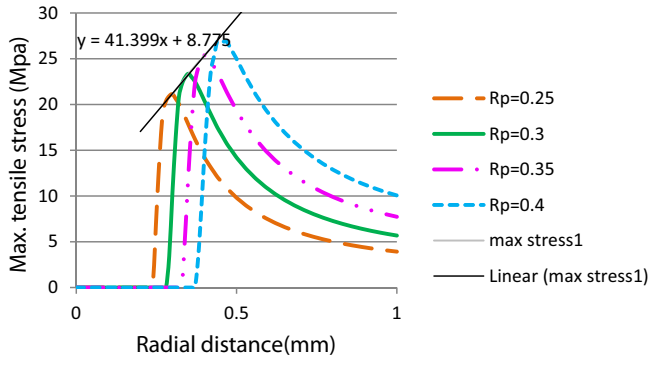


**Fig. 15.** Maximum tensile stress S1 for different particle sizes with power density $P_d = 10^{11}$ W/m$^3$ with exposure time $t = 0.0007$ s.

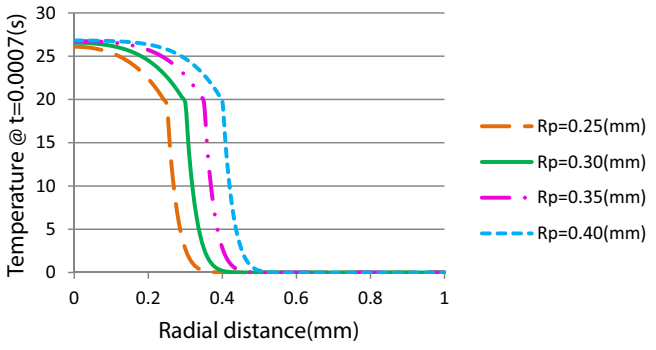


**Fig. 16.** Temperature profiles for different particle sizes under power density $P_d = 10^{11}$ W/m$^3$ with exposure time $t = 0.0007$ s.

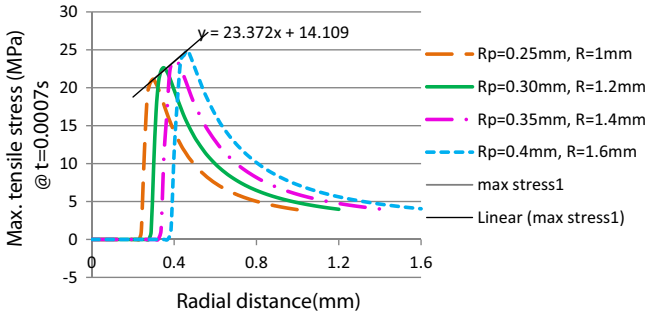


**Fig. 17.** Maximum tensile stress for different particle sizes but the same ratio of $R_p/R = 0.25$ with power density $P_d = 10^{11}$ W/m$^3$ in time $t = 0.0007$ s.

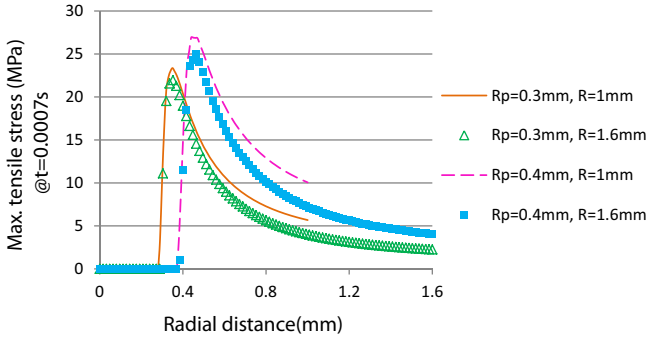


**Fig. 19.** Maximum tensile stress for same particle size $R_p = 0.30$ or 0.40 mm with a different size of calcite matrix ($R = 1$ and 1.6 mm) under power density $P_d = 10^{11}$ W/m$^3$ in time $t = 0.0007$ s.

Therefore, this conclusion confirms that short pulses of a high power density are effective and economical. In Fig. 3, with the exposure time of 0.0007 s, the maximum value of maximum tensile stress is 21 MPa, which is high enough to produce cracks in the pyrite.

On the other hand, if the exposure time remained at $t = 0.0007$ s and the power densities changed from $10^8$ W/m$^3$ to $10^{11}$ W/m$^3$, Fig. 9 demonstrates that the location of maximum stress does not change. The conclusion is that the location of maximum stress was related to exposure time and the shorter the time, the closer the initial cracks will be to the interface of the minerals. Conversely, longer times allow thermal diffusion in calcite and induce a compressive stress that decreases the tensile stress due to the thermal expansion of the pyrite.

In Fig. 9 the maximum tensile stresses with power densities less than $10^{10}$ W/m$^3$ are much smaller than when the power densities are under $10^{11}$ W/m$^3$. This result is consistent with the conclusion from D. A. Jones et al. (Jones et al., 2005), who stated that below $10^{10}$ W/m$^3$ very little heating occurs.

Conclusions in this section are very consistent with the results from Salsman et al. (1996) and Wang and Forssberg (2005). According to their experimental results the rise in temperature is relatively slow at lower microwave energy intensity, but increasing the energy intensity substantially shortens the time scale over which significant heating occurs and provides a sharper temperature gradient, which will create correspondingly large stress gradients.

### 4.3. Crack modelling

Previous work shows that microwaves can thermally fracture materials and enhance mineral liberation, but the actual mechanisms associated with such benefits are difficult to determine and predict. By means of the commercial software ANSYS, the thermal results of microwave heating can be calculated, but the breakage process due to the microwave heating cannot be simulated in this software. A numerical thermal fracture model has been developed at the JKMRC, the SimRock software

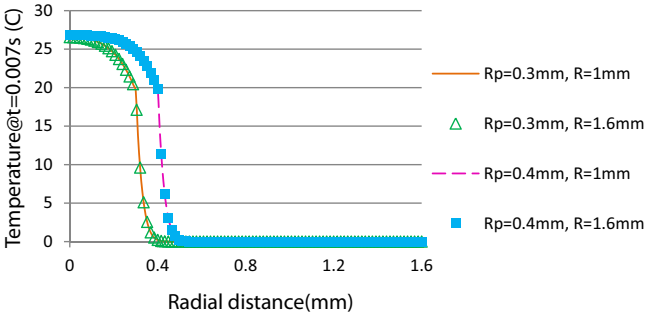


**Fig. 18.** Temperature for same particle size $R_p = 0.30$ or 0.4 mm with a different size of calcite matrix ($R = 1$ and 1.6 mm) under power density $P_d = 10^{11}$ W/m$^3$ in time $t = 0.0007$ s.

(Wang, 2013), in which a texture-based finite element method (FEM) modelling technique is used to present a realistic modelling method for characterizing the heterogeneous rock breakage behaviour according to its actual microstructure using integrated microscopic observation. Using the heat transfer analysis in SimRock, the cracks developed due to the thermal mismatch were simulated. Firstly the results of thermal stresses are compared with those of ANSYS, and the process of crack development is simulated based on the finite element method.

A simulation was performed on a sample with dimensions of $R_p = 0.5$ mm and $R = 1$ mm. A power density $P_d = le^{11}$ W/m$^3$ was applied to the sample for a time $t = 0.00045$ s to explore microwave heating. Using the commercial software ANSYS, the temperature distributions and the principle stresses were calculated. Under the same temperature distribution on the sample, the entire thermal cracking process (initiation, propagation and linkage of cracks) was simulated using SimRock.

Comparing the results in Figs. 10 and 11, it can be seen that the SimRock results of thermal stress (maximum stress = 21.4 MPa) are very close to those of ANSYS (maximum stress = 21.3 MPa). Fig. 12 shows the result of the SimRock cracking model using the finite element method.

Fig. 13 shows the maximum tensile stress in different exposure times. When exposure time $t = 0.00044$ s, the maximum value of stress approaches the tensile strength limit of 20 MPa.

Fig. 14 shows the development of cracks from an exposure time of $t = 0.00043$ s to $t = 0.0005$ s. As mentioned earlier, the damage is mainly caused by tensile stress, so the cracks develop in a radial direction. These conclusions had been obtained by D. A. Jones et al. as early as 2005 (Jones et al., 2005).

### 4.4. Particle size

In mineral processing, particle size plays a very important role. Several different grain sizes were tested. In Figs. 15 and 16, the radius of the pyrite grains ranged from 0.25 mm to 0.4 mm (taking the values $R_p = 0.25, 0.3, 0.35, 0.4$ mm) and the size of the calcite matrix remained the same ($R = 1$ mm). Power density and exposure time were also kept the same. The results show that peak stresses increased proportionally with the pyrite grain size, but the peak values of temperature changed little.

Keeping the ratio of $R_p/R$ the same ($R_p/R = 0.25/1, 0.3/1.2, 0.35/1.4, 0.4/1.6$) was considered, with the same power density $P_d = 10^{11}$ W/m$^3$ and time $t = 0.0007$ s. From Fig. 17, it can be seen that the slope of the peak line is smaller than the value in Fig. 15, which means that the size of calcite also affects the peak value of the stresses.

Additionally, the results of two models were compared. Each pair contained the same sized particle with different sizes of calcite matrix ($R = 1$ or 1.6 mm). The results were compared individually under the

same power density $10^{11}$ W/m$^3$ with an exposure time $t = 0.0007$ s. Figs. 18 and 19 show that the temperatures of each pair were exactly the same with a different size of matrix, but the maximum tensile stress of the large calcite matrix was lower than that of the smaller matrix size, because more thermal energy is needed in calcite to reach a thermal equilibrium state. Indeed the size of the calcite matrix affected the result of thermal stress; the smaller the particle size, the less the effect produced by the matrix size.

## 5. Conclusions

In this paper, the thermal cracking process around a single inclusion has been simulated numerically by the finite element method, and the dependence of the failure mechanism on power density and exposure time has been studied.

Results demonstrate that microwave energy has potential in mineral processing. From an economic standpoint, a high power density combined with a short heating interval is expected to offer the best energy efficiency.

The initial breakage is caused by tensile thermal stresses therefore cracks propagate gradually in a radial direction from the calcite matrix.

Cracks in the calcite matrix started close to the pyrite–calcite interface but not right on it. The main factor affecting the location of maximum stress was the thermal expansion of the calcite matrix, which in turn depends on the exposure time. The longer the exposure time, the further away the peak stress is from the interface of the different minerals.

The thermal expansion coefficient of the microwave-absorbing mineral (Pyrite) plays a critical role in producing thermal stresses and the location of initial cracking can be affected by the thermal property of the low-absorbing mineral (Calcite).

The breakage results are also affected by the proportion of microwave-absorbing minerals and lower-absorbing minerals. Larger pyrite grain sizes increase the peak stress, while larger matrix sizes reduce it.

## Acknowledgements

The work described in this paper was performed as part of the project of AMIRA GeM P843 and the funding for the research was provided by Anglo American and Rio Tinto.

## References

Amankwah, R.K., Khan, A.U., Pickles, C.A., Yen, T.T., 2005. Improved grindability and gold liberation by microwave pre-treatment of a free-milling gold ore. Miner. Process. Extr. Metall. (Trans. Inst. Miner. Metall. C) 114, 30–36.
Chen, T.T., Dutrizac, J.E., Hague, K.E., Wyslovzil, W., Kashyap, S., 1984. The relative transparency of minerals to microwave radiation. Can. Metall. Q. 23 (3), 349–351.
Fitzgibbon, K.E., Veasey, T.J., 1990. Thermally assisted liberation — a review. Miner. Eng. 3, 181–185.
Haque, K.E., 1999. Microwave energy for mineral treatment processes—a brief review. Int. J. Miner. Process. 57, 1–24.
Holman, B.W., 1926. Heat treatment as an agent in rock breaking. Trans. IMM 36, 219.
Jones, D.A., Lelyveld, T.P., Mavrofidis, S.D., Kingman, S.W., Miles, N.J., 2002. Microwave heating applications in environmental engineering—a review. Resour. Conserv. Recycl. 34, 75–90.
Jones, D.A., Kingman, S.W., Whittles, D.N., Lowndes, I.S., 2005. Understanding microwave assisted breakage. Mineral Engineering 18, 659–669.
Kingman, S.W., Rowson, N.A., 1998. Microwave treatment of minerals—a review. Minerals Eng. 11 (11), 1081–1087.
Lindroth, D.P., Podnieks, E.R., 1988. 18th Lunar and Planetary Science Conference, PLI, Houston, TX, pp. 365–373.
Raddatz, A.E., Walkiewicz, J.W., McGill, S.L., 1989. Microwave induced fracturing to improve grindability. Proceedings of the SAG Conference, Vancouver, Canada, pp. 503–512.
Rowson, N.A., Rice, N.M., 1990. Magnetic enhancement of pyrite by caustic microwave treatment. Miner. Eng. 3 (3/4), 363–368.
Salsman, J.B., Williamson, R.L., Tolley, W.K., Rice, D.A., 1996. Short-pulse microwave treatment of disseminated sulphide ores. Miner. Eng. 9 (1), 43–54.
Satish, H., Ouellet, J., Raghavan, V., Radziszewisi, P., 2006. Investigating microwave assisted rock breakage for possible space mining application. Min. Technol. 115, 34–40.
Schwechten, D., Milburn, G.H., 1990. Experiences in dry grinding with high compression roller mills for end product quality below 20 microns. Miner. Eng. 3 (1/2), 23–34.
Uslu, T., Atalay, Ü., Arol, A.I., 2003. Effect of microwave heating on magnetic separation of pyrite. Colloids Surf. A Physicochem. Eng. Asp. 225 (1/3), 161–167.
Walkiewicz, J.W., Clark, A.E., MgGill, S.L., 1991. Microwave-assisted grinding. IEEE Trans. Ind. Appl. 27 (2), 239–243.
Wang, Y., 2013. Numerical modelling of inhomogeneous rock breakage behaviour based on texture images. Computational Modelling '13. Falmouth, UK, June 18–19 2013.
Wang, Y., Forssberg, E., 2005. Dry comminution and liberation with microwave assistance. Scandinavian Journal of Metallurgy 34, 57–63.
Wills, B.A., Parker, R.H., Binns, D.G., 1987. Thermally assisted liberation of cassiterite. Miner. Metall. Process. 4 (2), 94–96.
Yates, A., 1918. Effect of beating and quenching Cornish tin ores before crushing. Trans. IMM 28, 41.